HHS Public Access

Author manuscript

Cell Microbiol. Author manuscript; available in PMC 2019 June 01.

Published in final edited form as:

Cell Microbiol. 2018 June ; 20(6): e12830. doi:10.1111/cmi.12830.

Cryptosporidium parvum disrupts intestinal epithelial barrier function via altering expression of key tight junction and adherens junction proteins

Anoop Kumar, **Ishita Chatterjee**, **Arivarasu N. Anbazhagan**, **Dulari Jayawardena**, **Shubha Priyamvada**, **Waddah A. Alrefai**, **Jun Sun**, **Alip Borthakur***, and **Pradeep K. Dudeja**

Division of Gastroenterology & Hepatology, Department of Medicine, UIC, and Jesse Brown VA Medical Center, Chicago IL 60612

Abstract

Infection with the protozoan parasite *Cryptosporidium parvum* (CP) causes cryptosporidiosis, a widespread diarrheal disease. Impaired intestinal epithelial barrier function and increased permeability are most commonly associated with diarrheal diseases caused by enteric infections. However, studies on barrier disruption and underlying mechanisms in cryptosporidiosis are extremely limited. Epithelial tight junctions (TJ) and adherens junctions (AJ) are important in maintaining barrier integrity. Therefore, we examined the effects of CP infection on paracellular permeability and on the expression of the major TJ and AJ proteins utilizing in vitro, ex vivo, and in vivo models. CP infection (0.5×10^6 oocysts/well in Transwell inserts, 24 h) increased paracellular permeability (FITC-dextran flux) in Caco-2 cell monolayers and substantially decreased the protein levels of occludin, claudin 4 and E-cadherin. Claudin 3, zonula occludens-1 (ZO1) and α-catenin were also significantly decreased, whereas claudin 1 and 2 and β-catenin were not altered. Substantial downregulation of occludin, claudin 4 and E-cadherin was also observed in response to CP infection ex vivo in mouse enteroid-derived monolayers, and in vivo in the ileal and jejunal mocosa of C57BL/6 mice. The mRNA levels of these proteins were also significantly decreased in CP infected mouse ileum and jejunum, but were unaltered in Caco-2 cells. Further, bafilomycin, an inhibitor of lysosomal proton pump, partially abrogated CP effects on occludin expression in Caco-2 cells, suggesting a potential role of posttranslational mechanisms, such as induction of protein degradation pathways, in mediating the effects of the parasite. Our studies suggest that disruption of barrier function via downregulation of specific key components of TJ and AJ could be a major mechanism underlying CP infection-induced diarrhea.

1 INTRODUCTION

The protozoan parasite *Cryptosporidium* species infects the epithelial cells of the small intestine to cause cryptosporidiosis, a widespread diarrheal disease, increasingly being recognized as an alarming global health problem (Checkley et al., 2015; Shirley, Moonah, &

*Author to whom all correspondence including reprint requests should be addressed: Alip Borthakur, Ph.D., Department of Medicine Division of Gastroenterology & Hepatology, University of Illinois at Chicago, 840 South Wood Street, MC 716, Chicago, IL 60612, alipb@uic.edu.

Conflict of Interests: All authors declare that there is no conflict of interests.

Kotloff, 2012; Shoultz, de Hostos, & Choy, 2016; Sparks, Nair, Castellanos-Gonzalez, & White, 2015). The Global Enteric Multicenter Study (GEMS) (Kotloff et al., 2013), and most recently a global network study of malnutrition and enteric diseases (MAL-ED) (Platts-Mills et al., 2015) reported this neglected parasite as 1 of the 4 major enteric pathogens causing life-threatening diarrhea in infants associated with growth stunting, high mortality and morbidity. Oocysts of the parasite entering human hosts via fecal-oral route invade the epithelial cells of the small intestine and reproduce on the apical surface of the epithelium. Cryptosporidiosis is now viewed as an important cause of diarrheal diseases in children and adults worldwide. In immunocompromized patients, such as those with AIDS, cryptosporidiosis can lead to persistent diarrhea and even death (Ryan & Hijjawi, 2015; Shirley et al., 2012; Ward, 2017). In developing countries, persistent infections with *Cryptosporidium* intensified by malnutrition have been associated with impaired physical and cognitive development in children (Checkley et al., 2015). Despite being recognized as a global health problem, however, treatment options for cryptosporidiosis are severely limited primarily due to lack of understanding of the mechanisms of *Cryptosporidium*-induced diarrhea.

Diarrheal diseases caused by enteric infections could involve impaired epithelial barrier function (Guttman & Finlay, 2009; Viswanathan, Hodges, & Hecht, 2009) as well as dysregulation of fluid and ion transport processes (Field, 2003; Hoque, Chakraborty, Sheikh, & Woodward, 2012). Intestinal epithelial barrier defects occur mostly via disruption of epithelial junctional complexes (AJC) such as tight junctions (TJ) and adherens junctions (AJ) (Guttman & Finlay, 2009; Mehta, Nijhuis, Kumagai, Lindsay, & Silver, 2015; Shen, Su, & Turner, 2009; Viswanathan et al., 2009). TJ provide the barrier required for the maintenance of the electrochemical gradients necessary for efficient transcellular ion transport (Viswanathan et al., 2009) whereas AJ serve as mechanical linkage between adjacent epithelial cells (France & Turner, 2017). These junctions comprise a variety of transmembrane proteins, coupled with cytoplasmic adaptor proteins and the actin cytoskeleton, to attach adjacent cells together thereby forming intercellular seals (France & Turner, 2017). Breaching of this barrier has profound effects on human health and disease, as barrier defects have been linked with the onset of inflammation, diarrhea and other extra-intestinal effects. Various enteric pathogens have developed specific strategies to alter or disrupt these structures as part of their pathogenesis, resulting in either pathogen invasion, or other consequences such as diarrhea (Guttman & Finlay, 2009; Vogelmann, Amieva, Falkow, & Nelson, 2004). Understanding the strategies that microorganisms use to commandeer the functions of AJC defines an important area of research in microbial pathogenesis (Guttman & Finlay, 2009).

Few earlier studies showed decreased transepithelial resistance and increased paracellular permeability following *C. parvum* infection of intestinal epithelial cells in vitro or in vivo (Di Genova & Tonelli, 2016; Roche, Martins, Cosme, Fayer, & Guerrant, 2000). However, very little is known about the mechanisms of impaired barrier function or the effects on the expression of TJ and AJ assembly proteins in response to *Cryptosporidium* infection.

Our current studies demonstrated decreased expression of specific TJ and AJ assembly proteins in response to *C. parvum* infection that could contribute, at least partially, to disruption of barrier function and associated diarrhea.

2 RESULTS

2.1 Time-course of *C. parvum* invasion of Caco-2 monolayers

We measured time-course of cellular entry of excysted oocysts (sporozoits) of *C. parvum* (CP) by direct immunofluorescence labeling of the parasite with Sporo-Glo reagent (Waterborne Inc, New Orleans, LA) following manufacturer's instructions. As shown in Figure 1, the parasite was stained intracellularly as early as 4 hrs following treatment from apical surface of transwell grown Caco-2 monolayers, with cellular entry gradually increasing till 24 hrs. However, virtually there was no cellular entry of the parasite even after 24 hrs when oocysts were added from basolateral side. For all the subsequent experiments in Caco-2 cells and mouse enteroid monolayers, parasite treatment was given from the apical surface for 24 hrs.

2.2 *C. parvum* infection increases paracellular permeability in Caco-2 monolayers

Measurement of apical to basolateral flux of FITC dextran was used to assess the CP infection effects on paracellular permeability in transwell-grown confluent Caco-2 monolayers. As shown in Figure 2, CP infection of Caco-2 monolayers from apical surface for 24 hr caused a 3-fold increase in FITC-dextran flux compared to untreated monolayers.

2.3 Differential effects of *C. parvum* infection on the expression of TJ and AJ proteins

The intercellular apical junctional complex (AJC) (France & Turner, 2017; Ivanov, Parkos, & Nusrat, 2010) regulates epithelial barrier function, permitting the passive entry of nutrients, ions, and water, while restricting pathogen access to underlying tissue compartments. The most apical tight junction (TJ) and its subjacent adherens junction (AJ) constitute the AJC. Since TJ and AJ are common targets of most enteric pathogens, we sought to examine the effects of CP infection on the expression of key proteins that comprise TJ and AJ assembly. As shown in Figure 3A, *C. parvum* infection of Caco-2 cells substantially decreased the protein levels of occludin and claudin 4, the TJ proteins. Although to a relatively lesser extent, the protein levels of claudin 3 and of the adaptor protein ZO1 were also significantly decreased. However, CP infection did not alter claudin 1 and claudin 2. *C. parvum* infection effects on AJ components are shown in Figure 3B. As evident, there was extensive downregulation of E-cadherin, a key component of AJ. Level of α-catenin, an AJ-associated protein, was significantly decreased, whereas there was no effect on β-catenin. We also measured the levels of occludin, claudin 4 and E-cadherin by immunofluorescence staining of the proteins in transwell grown mouse enteroid-derived monolayers following CP infection for 24 hours. Similar to the results obtained in Caco-2 cells, CP infection substantially decreased immunostaining intensity of these proteins in mouse enteroids (Figure 3C). We next examined the mRNA levels of occludin, claudin 4 and E-cadherin, the TJ/AJ proteins that were substantially downregulated by CP infection in Caco-2 cells. As shown in Figure 3D, CP infection did not alter the mRNA levels of these proteins.

2.4 *C. parvum* infection decreases mRNA and protein levels of occludin, claudin 4 and E-cadherin in mouse ileum and jejunum

We next utilized in vivo model of CP infection in C57BL/6 mice to examine the effects on the expression of the key TJ and AJ proteins that were maximally downregulated in Caco-2 cells in response to infection by the parasite. Mice were infected with 1×10^7 oocysts/mouse by oral gavage for 24 and 48 hrs. Unlike in Caco-2 cells, mRNA levels of occludin, claudin-4 and E-cadherin were significantly decreased in the mouse ileum and jejunum (Figure 4A) whereas there was no significant change in claudin 2 mRNA. We also measured protein levels of occludin, claudin 4 and E-cadherin by immunoblotting and/or immunofluorescence staining. CP infection decreased occludin and claudin 4 protein levels (Figure 4B) and immunostaining of occludin, claudin 4 and E-cadherin (Figure 4C) in immunofluorescence studies.

2.5 Effects of *C. parvum* infection on cytokine levels and myeloperoxidase (MPO) activity in mouse ileum

In order to assess whether CP-induced alterations in the expression of TJ/AJ proteins at 24 hr post-infection was secondary to mucosal inflammation, we measured mRNA levels of key cytokines and MPO activity in ileal mucosa. As shown in Figure 5A, mRNA levels of TNF-α and IFN-γ were significantly increased whereas there were no significant effects on mRNA levels of IL-1β, IL-6, CXCL1 and COX2 in response to CP infection for 24 hr. Further, there was no effect of CP infection on MPO activity (Figure 5B), a measure of mucosal infiltration of neutrophils and marker of inflammation, in the mouse ileal mucosa. H&E staining (Figure 5C) of infected versus control ileal mucosa also did not show marked changes in cellular morphology in response to CP infection. Further, although previous studies have shown decreased barrier function in response to TNF-α and IFN-γ (Al-Sadi, Guo, Ye, & Ma, 2013; Capaldo & Nusrat, 2009), these changes did not involve downregulation of expression of TJ/AJ proteins. Overall, our results could suggest that decreased expression of specific AJC proteins in mouse ileum in response to CP infection for 24 hr was not primarily due to inflammation.

2.6 *C. parvum* infection induces apoptosis in mouse ileum

Previous studies have shown *C. parvum* induction of apoptosis of intestinal epithelial cells that was attributed to altered barrier function (Foster, Stauffer, Stone, & Gookin, 2012; Laurent & Lacroix-Lamande, 2017; McCole, Eckmann, Laurent, & Kagnoff, 2000). We examined the occurrence of apoptosis in the ileal mucosa in response to *C. parvum* infection of mice via measurement of the levels of cleaved caspase-3. As shown in Figure 6, *C. parvum* infection for 24 hr significantly increased the level of cleaved caspase-3 in the ileal mucosa, suggesting occurrence of apoptosis.

2.7 Bafilomycin A alleviates *C. parvum*-induced downregulation of occludin in Caco-2 cells

Since CP infection substantially decreased occludin protein levels in Caco-2 cells, but had no effects on occludin mRNA, we examined the role of posttranslational mechanisms, such as protein degradation pathways, in mediating CP-induced downregulation of occludin protein in Caco-2 cells. Ubiquitin-proteosomal system and lysosomal degradation are two

cornerstones of cellular catabolism involved in intracellular protein degradation under normal physiology or in a broad array of pathological states (Korolchuk, Menzies, & Rubinsztein, 2010). Therefore, we utilized pharmacological inhibitors of these pathways to examine if CP infection triggered any of these pathways to degrade cellular occludin. Our results showed that bafilomycin, an inhibitor of lysosomal proton pump, partially abrogated CP-induced downregulation of occludin expression (Figure 7), whereas MG132, a proteosomal inhibitor, had no effect. These results suggest that CP induction of specific protein degradation pathways, at least partially, could account for its effects in downregulating occludin expression.

2.8 *C. parvum* infection decreases low MW form of Triton X 100-insoluble occludin

Occludin has been shown to partition into both Triton X-100-soluble and -insoluble fractions (Andreeva, Krause, Muller, Blasig, & Utepbergenov, 2001; Nusrat et al., 2001). Because of different levels of phosphorylation, occludin exhibits a molecular weight in the range of 65–80 kDa on Western blot (Andreeva et al., 2001; Farshori & Kachar, 1999). A high molecular weight form of occludin, reflecting enhanced phosphorylation, appears only in the Triton X-100-insoluble fraction. The decreased expression of occludin in CP infected cells reported above (Figure 3A) prompted us to examine whether infection also alters the distribution of the protein in the Triton X-100-soluble and -insoluble fractions. As shown in Figure 8, occludin showed a strong band of about 65 kDa [low MW band] and a relatively weaker band of ~78 kDa (hight MW band representing hyperphosphorylated form) in the detergent-insoluble fraction of uninfected Caco-2 cells. Densitometric analysis showed 50–60% decrease in the levels of the low MW form of occludin in the detergent-insoluble fraction in the CP infected cells compared to those in uninfected controls, whereas the level of the high MW phosphorylated form was not significantly altered (Figure 8). Occludin level in the detergent-soluble fraction that showed a single band at 65 kDa was much lower and CP infection did not seem to have any significant effect on occludin level in this fraction.

3 DISCUSSION

The objective of this study was to examine the mechanisms underlying disruption of intestinal epithelial barrier function in response to infection by *Cryptosporidium parvum*. Infection by this parasite in immunocompetent hosts may cause acute, self-limiting or recurrent diarrhea, while in immunocompromized hosts it may lead to fulminant diarrhea, extra-intestinal manifestations, and death (Checkley et al., 2015; Ward, 2017). However, the molecular and cellular basis of *Cryptosporidium* infection-induced diarrhea is poorly understood. Persistent infectious diarrheal diseases commonly affect mucosal barrier that separate the luminal contents from the body's internal milieu. This barrier, the first line of defense against external pathogens, is formed by a monolayer of intestinal epithelial cells and the substances they secrete. This selectively permeable barrier prohibits passage of luminal microorganisms and their toxins while permitting flux of water, ions and solutes, including nutrients. The epithelium maintains its selective barrier function through the formation of complex protein-protein networks, collectively known as apical junctional complex (AJC) (Matter & Balda, 2003) that mechanically link adjacent cells and seal the intercellular space. The tight junctions (TJ) and adherens junctions (AJ) are key components

of AJC comprising transmembrane proteins that interact extracellularly with adjacent cells and intracellularly with adaptor proteins that link to the cytoskeleton (Groschwitz & Hogan, 2009). TJs seal paracellular gaps between adjacent epithelial cells (Tsukita, Furuse, & Itoh, 2001), whereas AJs are responsible for cell–cell contacts (Yap, Brieher, & Gumbiner, 1997). The TJ barrier exhibits both size and charge selectivity with two distinct routes across an intact epithelial monolayer, termed the 'pore' and 'leak' pathways (France & Turner, 2017). The pore pathway refers to a high-capacity, size-selective and charge-selective route, whereas the leak pathway is a low-capacity pathway that has more limited selectivity. Both TJ and AJ assemblies are under intricate homeostatic regulation under normal physiology and are known to be dysregulated in various disease states (France & Turner, 2017).

Several diarrheal pathogens have been shown to disrupt AJCs in in vitro and in vivo models of infection (Groschwitz & Hogan, 2009; Nusrat et al., 2001; Vogelmann et al., 2004). Although limited studies demonstrated disrupted barrier function in cryptosporidiosis (Di Genova & Tonelli, 2016; Roche et al., 2000), very little is known about the alterations in the expression and/or assembly of TJ and AJ proteins and the underlying mechanisms. Since *C. parvum* is known to infect and invade the cells of small intestinal epithelium, we used post-confluent Caco2 cell monolayers, morphologically and functionally mimicking the small intestinal mucosal barrier (Hidalgo, Raub, & Borchardt, 1989; Pignata, Maggini, Zarrilli, Rea, & Acquaviva, 1994), to examine the effects of infection by the parasite.

In order to gain molecular insights into *C. parvum*-induced increase in FITC-dextran flux, indicating increased paracellular permeability or disrupted barrier function, we analyzed the effects of infection on AJC components. We were able to show, for the first time, extensive downregulation of expression of the TJ proteins occludin and claudin 4, and of E-cadherin, a key component of AJ following *C. parvum* infection. Claudin 3 was also significantly decreased, whereas claudin 1 and 2 were not altered. ZO1, the adaptor protein that link TJ assembly to the actin cytoskeleton and is also known to regulate leak pathway permeability (France & Turner, 2017) was also significantly decreased in response to *C. parvum* infection. Similar to our observations in Caco-2 cells, occludin, claudin 4, and E-cadherin were extensively downregulated in *C. parvum* infected mouse enteroid-derived monolayers and in the ileal and jejunal mucosa of mice administered *C. parvum* for 24 and 48 hrs. It is important to note that in Caco-2 cells parasite infection had no effects on the mRNA levels of occludin, claudin 4 and E-cadherin, whereas both their mRNA and protein levels were decreased in vivo in mouse jejunum and ileum. This could signify differential regulatory mechanisms in different mammalian species or could be due to the fact that multiple factors come into play in the compositionally complex in vivo environment of the native intestine. In either case, however, it appears that posttranslational mechanisms, at least partially, are important in *C. parvum* infection-induced modulation of specific AJC protein expression. Indeed, our studies in Caco-2 cells further showed that bafilomycin A, an inhibitor of lysosomal proton pump, partially blocked the effects of *C. parvum* infection on occludin expression suggesting the role of parasite-induced protein degradation pathways in reducing occludin levels. Additional studies are needed to determine the relative contribution of lysosomal pathways of protein degradation and/or other posttranslational mechanisms employed by *C. parvum* in downregulating the expression of occludin and/or other TJ/AJ proteins.

The role of occludin in regulating tight junction integrity has been suggested from studies showing increased transepithelial resistance (improved barrier function) following overexpression of occudin (Balda et al., 1996). Occludin has also been shown to regulate paracellular pore and leak pathways via its effects on claudins (France & Turner, 2017). The role of occludin in barrier regulation is, nevertheless, controversial because two studies have reported normal intestinal barrier function in unstressed occludin-deficient mice (Saitou et al., 2000; Schulzke et al., 2005). It appears from various studies that occudin could be a regulator of tight junctions, rather than an essential component, an interpretation that could explain the absence of intestinal barrier defects in unstressed occudin-deficient mice (France & Turner, 2017). Previous studies have also reported that levels of high and low MW occludin differing in phosphorylation levels could change in response to infection by enteric pathogens (Beau, Cotte-Laffitte, Amsellem, & Servin, 2007; Fiorentino, Levine, Sztein, & Fasano, 2014). However, the levels of high MW form of the occludin in the detergent-insoluble fraction representing hyperphosphorylated occludin appeared to be unaltered in response to *C. parvum* infection.

Claudins, critical components of TJ assembly, comprise a family of at least 24 proteins, whose differential expression and properties are believed to determine the tissue-specific variations in electrical resistance and paracellular permeability of epithelia (Gunzel & Yu, 2013). Claudin proteins are fundamental components of TJ strands. The consensus view is that the structure of the TJ, which forms the barrier, comprises barrier enhancing claudins (such as claudin 4) that occlude the intercellular space and pore-forming claudins (such as claudin 2) that form channels supporting solute flow (France & Turner, 2017). Further, experimental evidence has shown that overexpression of claudin 4 increases while that of claudin 2 decreases transepithelial resistance (TER) in cultured epithelial cell monolayers. Conversely, increased claudin 2 and/or decreased claudin 4 have been reported to be associated with barrier disruption in response to inflammation and infection (Guttman & Finlay, 2009; Landy et al., 2016; Zhang, Wu, Xia, & Sun, 2013). In our studies, both in vitro and in vivo, *C. parvum* infection substantially decreased claudin 4, but showed no effects on claudin 2. Earlier studies have shown that claudin 4 expression reduces paracellular permeability only when claudin 2 is co-expressed, but not in monolayers lacking claudin 2 expression, suggesting that barrier enhancing claudins regulate paracellular permeability via antagonizing the function of pore-forming claudins (France & Turner, 2017). Therefore, although there was no effect on claudin 2 expression, *C. parvum* infection increased paracellular permeability presumably because the substantially reduced level of claudin 4 could not counteract the pore-forming function of basal levels of claudin 2.

Components of the adherens junction (AJ) provide a foundation for cell–cell interactions and are essential for tight junction assembly. The major component of the epithelial adherens junction is E-cadherin, a single-spanning transmembrane protein capable of homotypic cell–cell interactions. E-cadherin is used as a receptor for adhesion and/or internalization by several microorganisms, allowing microbial persistence in the host, avoidance of mechanical clearance, and increased pathogenesis (Costa, Leite, Seruca, & Figueiredo, 2013). Down-regulation of E-cadherin has been shown in response to infections with enteropathogenic bacteria and in the inflamed mucosa in Crohn's disease (Kucharzik, Walsh, Chen, Parkos, & Nusrat, 2001; Schneider et al., 2010). Decreased expression of E-

cadherin observed in our studies in response to *C. parvum* infection could contribute to barrier dysfunction and increased permeability. However, it remains to be determined whether impaired cell-cell interactions secondary to decreased E-cadherin facilitates parasite entry or is an after effect of cellular invasion.

Earlier studies have shown production of chemoattractants in response to *C. parvum* infection leading to immune cell infiltration to the site of infection (Laurent & Lacroix-Lamande, 2017). These studies, however, utilized longer time of infection (7–14 days) to examine the chronic effects, and some of the studies showing mucosal damage and neutrophil infiltration were in immunocompromized mice. Our current studies aimed at examining the early effects (24–48 hrs) of cryptosporidiosis on TJ and AJ proteins in immunocompetent mice did not show significant mucosal damage or immune cell recruitment to the mucosa during this early infection period. Thus, *C. parvum* infection seemed to reduce the expression of TJ/AJ proteins before initiation of any significant inflammatory response.

Various earlier studies have also shown induction of host cell apoptosis in response to *C. parvum* infection and implicated its relevance to epithelial barrier integrity (Foster et al., 2012; Laurent & Lacroix-Lamande, 2017; McCole et al., 2000). Whether the occurrence of apoptosis in cryptosporidiosis benefits the parasite or the host, however, is not clear (Sasahara et al., 2003). *C. parvum* has been shown to induce moderate apoptosis in vitro early after infection that was followed by induction of anti-apoptotic mechanisms via activation of NF-κB. These studies implicated that moderate levels of epithelial cell apoptosis could limit the host inflammatory response detrimental to the survival of the parasite. On the other hand, shedding of infected epithelial cells by apoptosis may benefit the host, since it allows maintenance of epithelial barrier integrity (McCole et al., 2000). Further studies utilizing caspase inhibitors will be needed to establish whether *C. parvum*-induced downregulation of key TJ/AJ proteins observed in our studies is a mechanism of disruption of barrier function independent of induction of apoptosis. In summary, our studies for the first time evaluated the molecular basis of disruption of epithelial barrier function in response to *C. parvum* infection via detailed analysis of the expression of TJ and AJ proteins that primarily regulate paracellular permeability. It has been suggested that subset of claudins including claudin 4 regulate pore pathway whereas leak pathway permeability is regulated by occludin and ZO1 (France & Turner, 2017). Therefore, increased paracellular permeability in response to *C. parvum* appears to signify alterations of both pore and leak pathways of permeability. Additional studies will be needed for elucidating the mechanisms underlying *C. parvum*-induced downregulation of specific TJ and AJ assembly proteins and the responses of host epithelial cells and their impact on barrier function. Further, effects of *C. parvum* infection on the proteins of desmosomes, another AJC component, remain to be investigated.

4 EXPERIMENTAL PROCEDURES

4.1 Chemicals and antibodies

RNeasy kits for RNA extraction were obtained from Qiagen (Valencia, CA), and real-time quantitative RT-PCR kits were obtained from Stratagene (La Jolla, CA). Antibodies for

occludin, claudins 1, 2, 3, 4, ZO1, α and β catenin were from Invitrogen (Carlsbad, CA) and for E-cadherin and caspase-3 were from Cell Signaling (Danvers, MA). Bafilomycin A and MG-132 were from Calbiochem (Burlington, MA), FITC-dextran was obtained from Sigma-Aldrich (St. Louis, MO).

4.2 Preparation of *Cryptosporidium* oocysts

Two major species of the parasite, viz. *C. parvum* and *C. hominis*, cause disease in humans (Ward, 2017). We have utilized *C. parvum* in our studies as this species, but not *C. hominis,* infects both human and mice. Suspensions of live oocysts of *C. parvum* in PBS were obtained from Waterborne Inc. (New Orleans, LA). For in vitro and ex vivo studies, oocysts were excysted by incubating 4 volumes of the suspension with 1 volume of 20% bleach solution for 10 min at room temperature. The pellet obtained by centrifugation was washed several times with HBSS to remove traces of bleach and finally resuspended in MEM cell culture media (Invitrogen) containing 0.2% taurocholate to release infectious sporozoites for treatments.

4.3 Cell culture

Caco-2 cells were obtained from American Type Culture Collection (ATCC, Manassas, VA) and grown at 37°C in a 5% CO_2-95% air environment. Cells were grown in MEM supplemented with 50 U/ml penicillin and 50 μg/ml gentamicin, and with 20% fetal bovine serum. For in vitro studies, cells were seeded on 6, 12 or 24-well plastic supports or 12-well transwell inserts and grown to confluency (12-days post-plating) before infecting with *Cryptosporidium* oocysts.

4.4 Mice

C57BL/6 mice (4–6 weeks old) obtained from Jackson Laboratories were maintained in the animal care facility of the Jesse Brown Veterans Affairs Medical Center (JBVAMC), Chicago. In vivo studies performed in these mice were approved by the Animal Care Committee of the University of Illinois at Chicago and JBVAMC. Mice were divided into 4 groups, 2 groups for infecting with *C. parvum* oocysts for 24 and 48 hr each and the other 2 groups being the respective controls. On day 1, each mouse in the 48 hr treatment group was gavaged with 1×10^7 intact (unexcysted) oocysts in 200 μl sterile PBS, whereas mice in the respective 48 hr control group received 200 μl of the vehicle. On day 2, mice in the 2 treatment groups (24 and 48 hr) were gavaged with 1×10^7 intact oocysts and the control groups with the vehicle. Mice were euthanized on 3^{th} day post CP infection. Intestines were resected, and mucosa was scraped for RNA extraction and lysate preparation. Sections (~2 μm) of the different regions of intestine (ileum and jejunum) were immediately snap-frozen in optimal cutting temperature embedding medium (Tissue-Tek OCT compound, Sakura) for immunofluorescence studies.

4.5 Preparation of crypt-derived mouse enteroids and enteroid-derived monolayers

Small intestinal crypt-derived enteroids from C57BL/6 mice were generated and cultured according to previously described protocol (Sato et al., 2011) with minor modifications. Briefly, small intestine was dissected and opened longitudinally and cut into small (~1 cm)

pieces after cleaning with ice-cold PBS (penicillin, 100 I.U./ml/streptomycin, 100 μg/ml). The tissues were rocked in PBS with 2 mM EDTA for 30 min at 4°C and then switched to PBS with 54.9 mM d-sorbitol and 43.4 mM sucrose. The tissues were then vortexed for 1–2 min and filtered through a 70 μm sterile cell strainer. The crypts were collected by centrifugation at 150*g* for 10 min at 4°C. Approximately 500 crypts were suspended in 50 μL growth factor reduced phenol-free Matrigel (BD Biosciences, San Jose, CA). Next, a 50 μL droplet of Matrigel/crypt mix was placed in the center of the well of a 12-well plate. After 30 min of polymerization, 650 μl of Mini gut medium (advanced DMEM/F12 supplemented with HEPES, L-glutamine, N2 and B27) was added to the culture, along with R-Spondin, Noggin, and EGF. The medium was changed every 2–3 days. For passaging, enteroids were removed from Matrigel and broken up mechanically by passing through a syringe and needle (27G, BD Biosciences), then transferred to fresh Matrigel. The passage was performed every 7–10 days with a 1:4 split ratio. For preparing enteroid-derived monolayers, enteroids were mechanically disrupted with a p1000 pipette and cultured as monolayers on Matrigels for 96 hrs as described previously (Sato et al., 2011) with minor modifications.

4.6 Determination of paracellular permeability

Paracellular permeability of the Caco-2 monolayers grown on 12-well transwell inserts (untreated or apically treated with 0.5×10^6 oocysts/well for 24 hr) was measured as apical to basolateral flux of FITC- Dextran (FD-4, M.W. 4 kDa; Sigma) as described previously (O'Hara, Feener, Fischer, & Buret, 2012).

4.7 Real-Time PCR

RNA was extracted from Caco-2 cells or homogenized mouse intestinal mucosal samples using Qiagen RNeasy kits. RNA was reverse transcribed and amplified using a Brilliant SYBR Green qRT-PCR Master Mix kit (Stratagene). Human and mouse TJ and AJ protein genes were amplified with gene-specific primers utilizing human and mouse GAPDH, respectively, as internal controls, as previously described by us (Kumar et al., 2016). Primer sequences of the genes used in this study are presented in Table 1.

4.8 Immunoblotting

Whole cell lysates (Caco-2) and mouse intestinal mucosal lysates were prepared as described previously by us (Kumar et al., 2016; Singh et al., 2014). Protein concentrations in the lysates were measured by the Bradford reagent (Bio-Rad, Hercules, CA). Protein extracts (50 μg of total proteins) were subjected to SDS-PAGE and transferred to nitrocellulose membranes. Levels of TJ/AJ proteins were immunodetected using specific antibodies and visualized by Enhanced Chemiluminescence reagents (ECL Plus; GE Healthcare, London, UK).

4.9 Immunofluorescence staining in mouse intestinal tissues

Sections of small intestinal tissues from different mice groups were snap frozen in optimal cutting temperature (OCT) embedding medium. For immunostaining, 5Wm frozen sections were fixed with 4% paraformaldehyde in PBS for 10 min at room temperature (RT). Fixed

sections were washed in PBS, permeabilized with 0.3% Nonidet P-40 for 5 min, sections were then encircled with water repellant pap pen (fisher) and blocked with 5% normal goat serum (NGS) for 1 hour at RT. Tissues were then incubated with the appropriate primary antibodies at a 1:100 ratio including anti-rabbit occludin (invitrogen), E-cadherin (cell signaling), claudin 4 (invitrogen) and anti-mouse villin (Invitrogen) in 1% NGS PBS for 2 hours at RT. After washing several times in PBS, sections were incubated with Alexa fluor-594-conjugated goat anti-rabbit IgG and Alexa Fluor 488-conjugated goat anti-mouse IgG (Invitrogen) at a ratio of 1:100 in 1 % NGS for 1 hour at RT. Sections were then washed in PBS and mounted under cover slips using Slowfade Gold antifade with DAPI reagent (Invitrogen). Sections were stored at −80°C until imaged. Images were acquired using Olympus BX51/1X70 fluoresence microscope equipped with X100 oil immersion objective.

4.10 Hematoxylin and eosin (H&E) staining and determination of myeloperoxidase activity

Cryopreserved mouse ileal tissues from each group were sectioned (5Wm) using a cryostat microtome. The sections were washed in PBS to remove excess OCT and fixed in 4% paraformaldehyde for 20 minutes. These tissues were washed again in PBS and stained with hematoxylin and eosin (H&E) stain kit from ScyTek Laboratories Inc. (Logan, UT) per the manufactures protocol. The slides were then mounted with permount (Fisher scientific, Waltham, MA) and stored at room temperature until use. Images from each group were acquired with Zeiss Axiocam acc1 microscope (Oberkochen, Germany) at 20 × magnifications. Myeloperoxidase (MPO) activity in the ileal mucosa was determined by the method of Krawisz et al (Krawisz, Sharon, & Stenson, 1984) with minor modifications. MPO activity was normalized to the amount of protein in the supernatant as measured by Bradford method and calculated as units per gram protein and expressed relative to control (considered as 100).

4.11 Immunoblotting of occludin in Triton X-100 soluble and insoluble fractions

Triton X-100 soluble and insoluble fractions were prepared as described previously (Fiorentino et al., 2014). Briefly, monolayers were harvested on ice in lysis buffer [1% Triton X-100, 100 mM NaCl, 10 mM HEPES, 2 mM EDTA, 4 mM Na_3VO_4, 40 mM NaF and a protease inhibitor cocktail (Complete Mini, Roche Molecular Biochemicals, Mannheim, Germany) and phosphatase inhibitors (Sigma)]. Lysates were rotated at 4°C, 30 min, centrifuged (14000 g for 30 min at 4°C) and the supernatant representing the Triton X-soluble fraction was collected. The remaining pellet was re-suspended in lysis buffer supplemented with 1% SDS and sonicated and centrifuged (14000 g for 5 min at 4°C). The supernatant, representing the Triton X-insoluble fraction, was collected. Samples were used immediately or stored at −80°C. Protein concentration was quantified by the Bradford method. Proteins in the samples were separated on SDS polyacrylamide gel and probed with anti-occludin antibody in immunoblotting.

4.12 Statistical Analyses

Data are presented as means ± SEM of 3–4 independent experiments. Differences between controls vs. treated groups were analyzed using one-way ANOVA with Tukey's test or Student’s t-test. Differences were considered significant at $P \leq 0.05$.

Acknowledgments

These studies were supported by; NIH (NIDDK): DK-54016, DK-81858, DK-92441 (PKD), DK-109709 (WAA); DK-105118 (JS); Senior Career Research Scientist Award (PKD), and Career Research Scientist Award (WAA) from the Department of Veteran Affairs; VA merit review grants: BX 002011 (PKD), BX 000152 (WAA); Bill & Melinda Gates Foundation: OPP1058288 (AB)

References

Al-Sadi R, Guo S, Ye D, Ma TY. TNF-alpha modulation of intestinal epithelial tight junction barrier is regulated by ERK1/2 activation of Elk-1. Am J Pathol. 2013; 183(6):1871–1884. DOI: 10.1016/j.ajpath.2013.09.001 [PubMed: 24121020]

Andreeva AY, Krause E, Muller EC, Blasig IE, Utepbergenov DI. Protein kinase C regulates the phosphorylation and cellular localization of occludin. J Biol Chem. 2001; 276(42):38480–38486. DOI: 10.1074/jbc.M104923200 [PubMed: 11502742]

Balda MS, Whitney JA, Flores C, Gonzalez S, Cereijido M, Matter K. Functional dissociation of paracellular permeability and transepithelial electrical resistance and disruption of the apical-basolateral intramembrane diffusion barrier by expression of a mutant tight junction membrane protein. J Cell Biol. 1996; 134(4):1031–1049. [PubMed: 8769425]

Beau I, Cotte-Laffitte J, Amsellem R, Servin AL. A protein kinase A-dependent mechanism by which rotavirus affects the distribution and mRNA level of the functional tight junction-associated protein, occludin, in human differentiated intestinal Caco-2 cells. J Virol. 2007; 81(16):8579–8586. DOI: 10.1128/JVI.00263-07 [PubMed: 17553883]

Capaldo CT, Nusrat A. Cytokine regulation of tight junctions. [Review]. Biochim Biophys Acta. 2009; 1788(4):864–871. DOI: 10.1016/j.bbamem.2008.08.027 [PubMed: 18952050]

Checkley W, White AC Jr, Jaganath D, Arrowood MJ, Chalmers RM, Chen XM, … Houpt ER. A review of the global burden, novel diagnostics, therapeutics, and vaccine targets for cryptosporidium. Lancet Infect Dis. 2015; 15(1):85–94. DOI: 10.1016/S1473-3099(14)70772-8 [PubMed: 25278220]

Costa AM, Leite M, Seruca R, Figueiredo C. Adherens junctions as targets of microorganisms: a focus on Helicobacter pylori. FEBS Lett. 2013; 587(3):259–265. DOI: 10.1016/j.febslet.2012.12.008 [PubMed: 23262219]

Di Genova BM, Tonelli RR. Infection Strategies of Intestinal Parasite Pathogens and Host Cell Responses. [Review]. Front Microbiol. 2016; 7:256.doi: 10.3389/fmicb.2016.00256 [PubMed: 26973630]

Farshori P, Kachar B. Redistribution and phosphorylation of occludin during opening and resealing of tight junctions in cultured epithelial cells. J Membr Biol. 1999; 170(2):147–156. [PubMed: 10430658]

Field M. Intestinal ion transport and the pathophysiology of diarrhea. J Clin Invest. 2003; 111(7):931–943. DOI: 10.1172/JCI18326 [PubMed: 12671039]

Fiorentino M, Levine MM, Sztein MB, Fasano A. Effect of wild-type Shigella species and attenuated Shigella vaccine candidates on small intestinal barrier function, antigen trafficking, and cytokine release. PLoS One. 2014; 9(1):e85211.doi: 10.1371/journal.pone.0085211 [PubMed: 24416363]

Foster DM, Stauffer SH, Stone MR, Gookin JL. Proteasome inhibition of pathologic shedding of enterocytes to defend barrier function requires X-linked inhibitor of apoptosis protein and nuclear factor kappaB. Gastroenterology. 2012; 143(1):133–144e134. DOI: 10.1053/j.gastro.2012.03.030 [PubMed: 22446197]

France MM, Turner JR. The mucosal barrier at a glance. [Review]. J Cell Sci. 2017; 130(2):307–314. DOI: 10.1242/jcs.193482 [PubMed: 28062847]

Groschwitz KR, Hogan SP. Intestinal barrier function: molecular regulation and disease pathogenesis. J Allergy Clin Immunol. 2009; 124(1):3–20. quiz 21–22. DOI: 10.1016/j.jaci.2009.05.038 [PubMed: 19560575]

Gunzel D, Yu AS. Claudins and the modulation of tight junction permeability. Physiol Rev. 2013; 93(2):525–569. DOI: 10.1152/physrev.00019.2012 [PubMed: 23589827]

Guttman JA, Finlay BB. Tight junctions as targets of infectious agents. Biochim Biophys Acta. 2009; 1788(4):832–841. DOI: 10.1016/j.bbamem.2008.10.028 [PubMed: 19059200]

Hidalgo IJ, Raub TJ, Borchardt RT. Characterization of the human colon carcinoma cell line (Caco-2) as a model system for intestinal epithelial permeability. Gastroenterology. 1989; 96(3):736–749. [PubMed: 2914637]

Hoque KM, Chakraborty S, Sheikh IA, Woodward OM. New advances in the pathophysiology of intestinal ion transport and barrier function in diarrhea and the impact on therapy. Expert Rev Anti Infect Ther. 2012; 10(6):687–699. DOI: 10.1586/eri.12.47 [PubMed: 22734958]

Ivanov AI, Parkos CA, Nusrat A. Cytoskeletal regulation of epithelial barrier function during inflammation. Am J Pathol. 2010; 177(2):512–524. DOI: 10.2353/ajpath.2010.100168 [PubMed: 20581053]

Korolchuk VI, Menzies FM, Rubinsztein DC. Mechanisms of cross-talk between the ubiquitin-proteasome and autophagy-lysosome systems. FEBS Lett. 2010; 584(7):1393–1398. DOI: 10.1016/j.febslet.2009.12.047 [PubMed: 20040365]

Kotloff KL, Nataro JP, Blackwelder WC, Nasrin D, Farag TH, Panchalingam S, … Levine MM. Burden and aetiology of diarrhoeal disease in infants and young children in developing countries (the Global Enteric Multicenter Study, GEMS): a prospective, case-control study. Lancet. 2013; 382(9888):209–222. DOI: 10.1016/S0140-6736(13)60844-2 [PubMed: 23680352]

Krawisz JE, Sharon P, Stenson WF. Quantitative assay for acute intestinal inflammation based on myeloperoxidase activity. Assessment of inflammation in rat and hamster models. Gastroenterology. 1984; 87(6):1344–1350. [PubMed: 6092199]

Kucharzik T, Walsh SV, Chen J, Parkos CA, Nusrat A. Neutrophil transmigration in inflammatory bowel disease is associated with differential expression of epithelial intercellular junction proteins. Am J Pathol. 2001; 159(6):2001–2009. DOI: 10.1016/S0002-9440(10)63051-9 [PubMed: 11733350]

Kumar A, Anbazhagan AN, Coffing H, Chatterjee I, Priyamvada S, Gujral T, … Dudeja PK. Lactobacillus acidophilus counteracts inhibition of NHE3 and DRA expression and alleviates diarrheal phenotype in mice infected with Citrobacter rodentium. Am J Physiol Gastrointest Liver Physiol. 2016; 311(5):G817–G826. DOI: 10.1152/ajpgi.00173.2016 [PubMed: 27634011]

Landy J, Ronde E, English N, Clark SK, Hart AL, Knight SC, … Al-Hassi HO. Tight junctions in inflammatory bowel diseases and inflammatory bowel disease associated colorectal cancer. World J Gastroenterol. 2016; 22(11):3117–3126. DOI: 10.3748/wjg.v22.i11.3117 [PubMed: 27003989]

Laurent F, Lacroix-Lamande S. Innate immune responses play a key role in controlling infection of the intestinal epithelium by Cryptosporidium. [Review]. Int J Parasitol. 2017; 47(12):711–721. DOI: 10.1016/j.ijpara.2017.08.001 [PubMed: 28893638]

Matter K, Balda MS. Signalling to and from tight junctions. Nat Rev Mol Cell Biol. 2003; 4(3):225–236. DOI: 10.1038/nrm1055 [PubMed: 12612641]

McCole DF, Eckmann L, Laurent F, Kagnoff MF. Intestinal epithelial cell apoptosis following Cryptosporidium parvum infection. Infect Immun. 2000; 68(3):1710–1713. [PubMed: 10678994]

Mehta S, Nijhuis A, Kumagai T, Lindsay J, Silver A. Defects in the adherens junction complex (E-cadherin/ beta-catenin) in inflammatory bowel disease. [Review]. Cell Tissue Res. 2015; 360(3): 749–760. DOI: 10.1007/s00441-014-1994-6 [PubMed: 25238996]

Nusrat A, von Eichel-Streiber C, Turner JR, Verkade P, Madara JL, Parkos CA. Clostridium difficile toxins disrupt epithelial barrier function by altering membrane microdomain localization of tight junction proteins. Infect Immun. 2001; 69(3):1329–1336. DOI: 10.1128/IAI.69.3.1329-1336.2001 [PubMed: 11179295]

O'Hara JR, Feener TD, Fischer CD, Buret AG. Campylobacter jejuni disrupts protective Toll-like receptor 9 signaling in colonic epithelial cells and increases the severity of dextran sulfate sodium-induced colitis in mice. Infect Immun. 2012; 80(4):1563–1571. DOI: 10.1128/IAI.06066-11 [PubMed: 22311925]

Pignata S, Maggini L, Zarrilli R, Rea A, Acquaviva AM. The enterocyte-like differentiation of the Caco-2 tumor cell line strongly correlates with responsiveness to cAMP and activation of kinase A pathway. Cell Growth Differ. 1994; 5(9):967–973. [PubMed: 7819134]

Platts-Mills JA, Babji S, Bodhidatta L, Gratz J, Haque R, Havt A, … Houpt ER. Pathogen-specific burdens of community diarrhoea in developing countries: a multisite birth cohort study (MAL-ED). Lancet Glob Health. 2015; 3(9):e564–575. DOI: 10.1016/S2214-109X(15)00151-5 [PubMed: 26202075]

Roche JK, Martins CA, Cosme R, Fayer R, Guerrant RL. Transforming growth factor beta1 ameliorates intestinal epithelial barrier disruption by Cryptosporidium parvum in vitro in the absence of mucosal T lymphocytes. Infect Immun. 2000; 68(10):5635–5644. [PubMed: 10992464]

Ryan U, Hijjawi N. New developments in Cryptosporidium research. Int J Parasitol. 2015; 45(6):367–373. DOI: 10.1016/j.ijpara.2015.01.009 [PubMed: 25769247]

Saitou M, Furuse M, Sasaki H, Schulzke JD, Fromm M, Takano H, … Tsukita S. Complex phenotype of mice lacking occludin, a component of tight junction strands. Mol Biol Cell. 2000; 11(12): 4131–4142. [PubMed: 11102513]

Sasahara T, Maruyama H, Aoki M, Kikuno R, Sekiguchi T, Takahashi A, … Inoue M. Apoptosis of intestinal crypt epithelium after Cryptosporidium parvum infection. J Infect Chemother. 2003; 9(3):278–281. DOI: 10.1007/s10156-003-0259-1 [PubMed: 14513402]

Sato T, Stange DE, Ferrante M, Vries RG, Van Es JH, Van den Brink S, … Clevers H. Long-term expansion of epithelial organoids from human colon, adenoma, adenocarcinoma, and Barrett's epithelium. Gastroenterology. 2011; 141(5):1762–1772. DOI: 10.1053/j.gastro.2011.07.050 [PubMed: 21889923]

Schneider MR, Dahlhoff M, Horst D, Hirschi B, Trulzsch K, Muller-Hocker J, … Kolligs FT. A key role for E-cadherin in intestinal homeostasis and Paneth cell maturation. PLoS One. 2010; 5(12):e14325.doi: 10.1371/journal.pone.0014325 [PubMed: 21179475]

Schulzke JD, Gitter AH, Mankertz J, Spiegel S, Seidler U, Amasheh S, … Fromm M. Epithelial transport and barrier function in occludin-deficient mice. Biochim Biophys Acta. 2005; 1669(1): 34–42. DOI: 10.1016/j.bbamem.2005.01.008 [PubMed: 15842997]

Shen L, Su L, Turner JR. Mechanisms and functional implications of intestinal barrier defects. Dig Dis. 2009; 27(4):443–449. DOI: 10.1159/000233282 [PubMed: 19897958]

Shirley DA, Moonah SN, Kotloff KL. Burden of disease from cryptosporidiosis. Curr Opin Infect Dis. 2012; 25(5):555–563. DOI: 10.1097/QCO.0b013e328357e569 [PubMed: 22907279]

Shoultz DA, de Hostos EL, Choy RK. Addressing Cryptosporidium Infection among Young Children in Low-Income Settings: The Crucial Role of New and Existing Drugs for Reducing Morbidity and Mortality. [Editorial]. PLoS Negl Trop Dis. 2016; 10(1):e0004242.doi: 10.1371/journal.pntd.0004242 [PubMed: 26820408]

Singh V, Kumar A, Raheja G, Anbazhagan AN, Priyamvada S, Saksena S, … Dudeja PK. Lactobacillus acidophilus attenuates downregulation of DRA function and expression in inflammatory models. Am J Physiol Gastrointest Liver Physiol. 2014; 307(6):G623–631. DOI: 10.1152/ajpgi.00104.2014 [PubMed: 25059823]

Sparks H, Nair G, Castellanos-Gonzalez A, White AC Jr. Treatment of Cryptosporidium: What We Know, Gaps, and the Way Forward. Curr Trop Med Rep. 2015; 2(3):181–187. DOI: 10.1007/s40475-015-0056-9 [PubMed: 26568906]

Tsukita S, Furuse M, Itoh M. Multifunctional strands in tight junctions. [Review]. Nat Rev Mol Cell Biol. 2001; 2(4):285–293. DOI: 10.1038/35067088 [PubMed: 11283726]

Viswanathan VK, Hodges K, Hecht G. Enteric infection meets intestinal function: how bacterial pathogens cause diarrhoea. Nat Rev Microbiol. 2009; 7(2):110–119. DOI: 10.1038/nrmicro2053 [PubMed: 19116615]

Vogelmann R, Amieva MR, Falkow S, Nelson WJ. Breaking into the epithelial apical-junctional complex--news from pathogen hackers. Curr Opin Cell Biol. 2004; 16(1):86–93. DOI: 10.1016/j.ceb.2003.12.002 [PubMed: 15037310]

Ward HD. New Tools for Cryptosporidium Lead to New Hope for Cryptosporidiosis. Trends Parasitol. 2017; doi: 10.1016/j.pt.2017.07.004

Yap AS, Brieher WM, Gumbiner BM. Molecular and functional analysis of cadherin-based adherens junctions. Annu Rev Cell Dev Biol. 1997; 13:119–146. DOI: 10.1146/annurev.cellbio.13.1.119 [PubMed: 9442870]

Zhang YG, Wu S, Xia Y, Sun J. Salmonella infection upregulates the leaky protein claudin-2 in intestinal epithelial cells. PLoS One. 2013; 8(3):e58606.doi: 10.1371/journal.pone.0058606 [PubMed: 23505542]

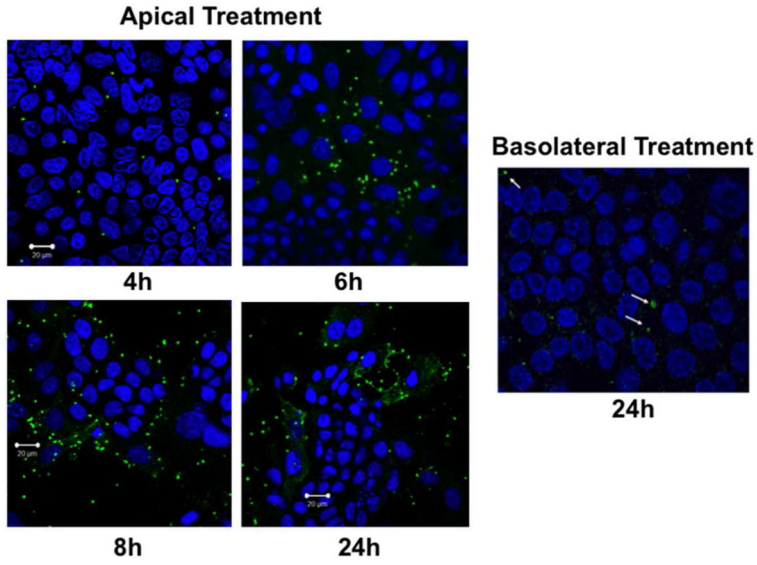

Figure 1.

Time-course of *C. parvum* invasion in Caco-2 cells. Post-confluent (12-day post-plating) Caco-2 monolayers grown on 12-well Transwell inserts were treated from apical or basolateral surfaces with 0.5×10^6 excysted oocysts (sporozoytes) of the parasite prepared as described in Methods. After 4, 6, 8 or 24 hr, monolayers were washed 3–4 times from both sides with 1×PBS to remove oocysts that did not enter the cells. Intracellular sporozoytes were then detected by direct immunofluorescence labeling with Sporo-Glo reagent. Representative images of 3 independent experiments are shown.

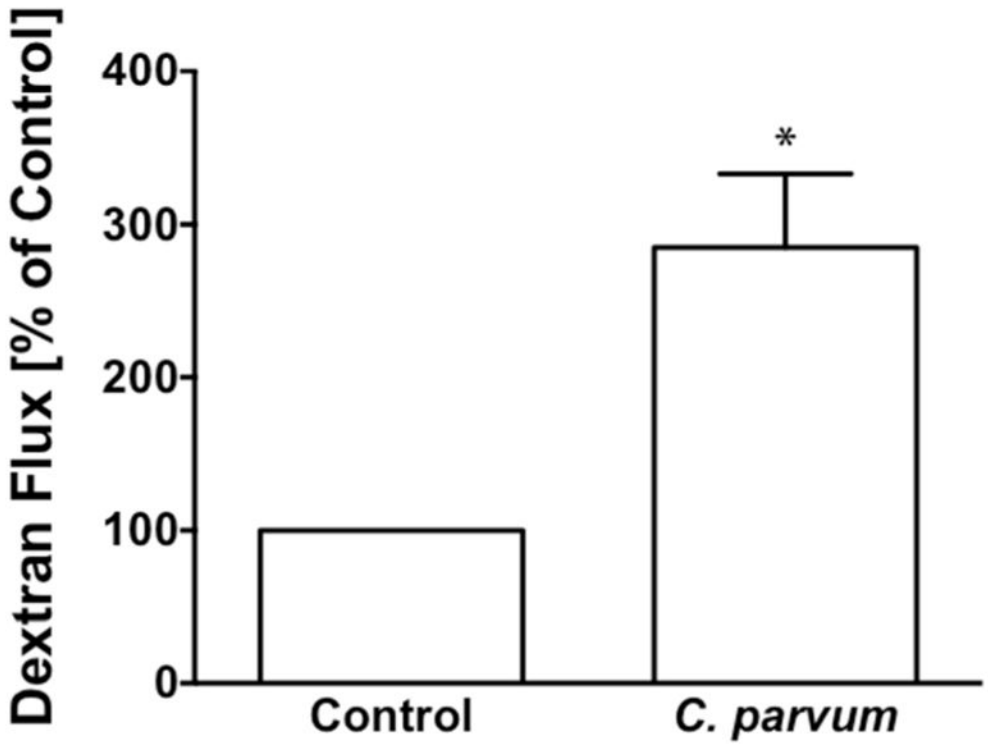

Figure 2.

C. parvum infection increases paracellular permeability in Caco-2 monolayer. Post-confluent Caco-2 monolayers grown on 12-well Transwell inserts were treated from apical surface with 0.5×10^6 sporozoytes for 24 hr. Paracellular permeability was measured as apical to basolateral flux of FITC- Dextran as described in Methods. Results expressed as percent of control represent mean ± SEM of 4 independent experiments. *P<0.05 vs. control.

Figure 3A

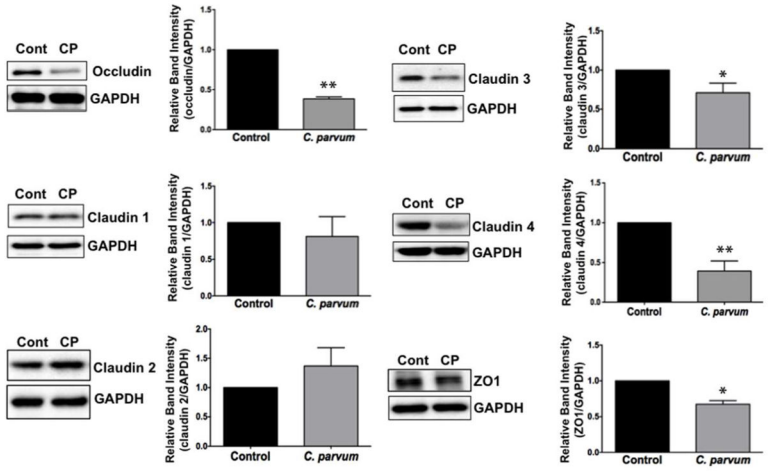

Figure 3B

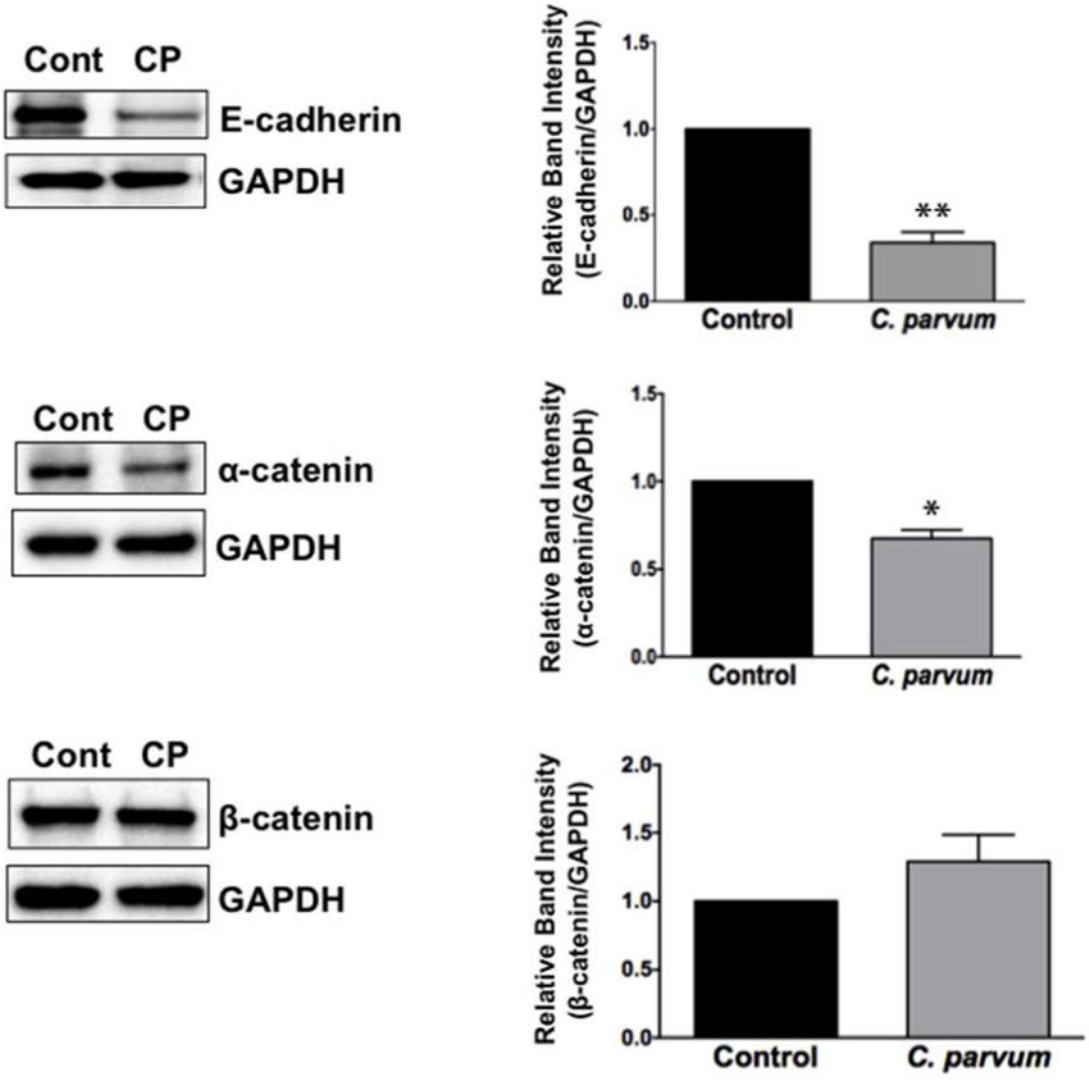

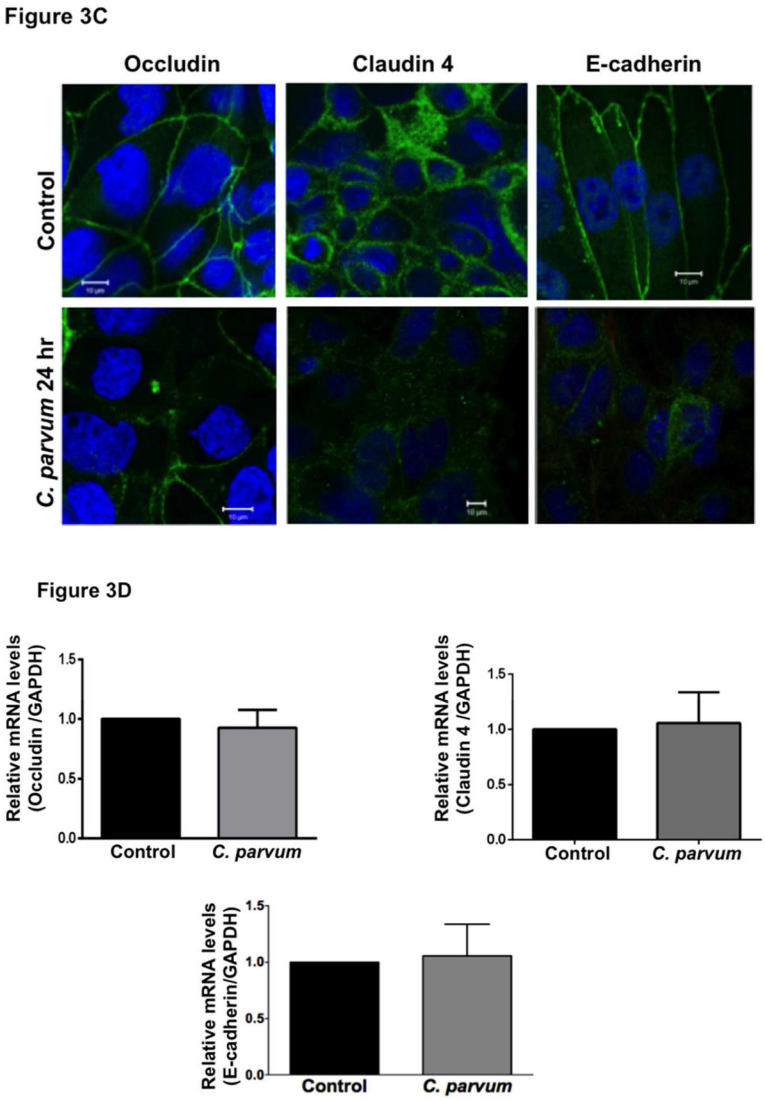

Figure 3.

Differential effects of *C. parvum* infection on mRNA and protein levels of TJ and AJ components in Caco-2 monolayers. Post-confluent Caco-2 monolayers grown on 24-well plastic supports were treated with 0.5×10^6 sporozoytes/well for 24 hr. Cell lysate was subjected to SDS-PAGE and probed with (A) antibodies for TJ proteins (occludin, claudin 1,2,3,4 and ZO1 and (B) antibodies for AJ proteins (E-cadherin, α- and β-catenin) in immunoblotting. GAPDH was used as the internal control. Densitometric analyses of band intensities are shown on right hand sides of each blot. Representative blots of 3–4 independent experiments are shown (**P*<0.05 vs. control; ***P*<0.001 vs. control). (C) Mouse ileal crypt-derived enteroids and enteroid-derived monolayers were prepared as described in Methods. Monolayers treated with *C. parvum* from apical surface for 24 hr were processed for immunofluorescence staining for occludin, claudin 4 and E-cadherin (green) and DAPI (blue). Representative images of 3 independent experiments are shown. (D) Relative mRNA abundance of occludin, claudin 4 and E-cadherin in total RNA samples

extracted from control or *C. parvum* treated Caco-2 cells was determined by real-time RT-PCR using gene-specific primers. GAPDH was used as an internal control. Values are mean ± SE of 4 separate experiments.

Figure 4A

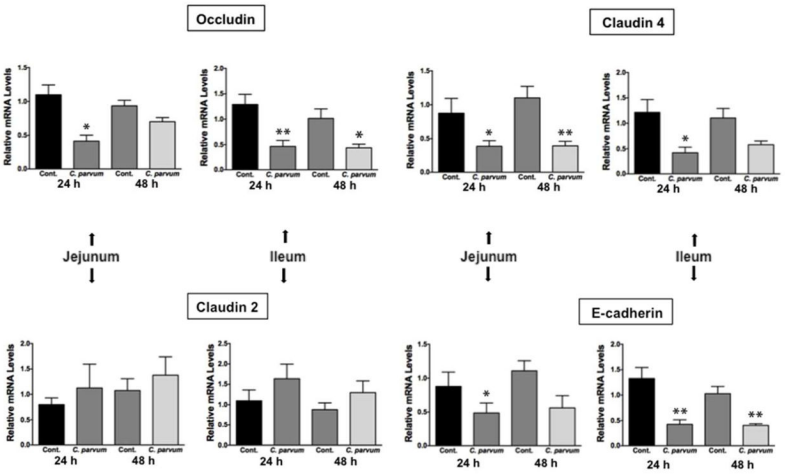

Figure 4B

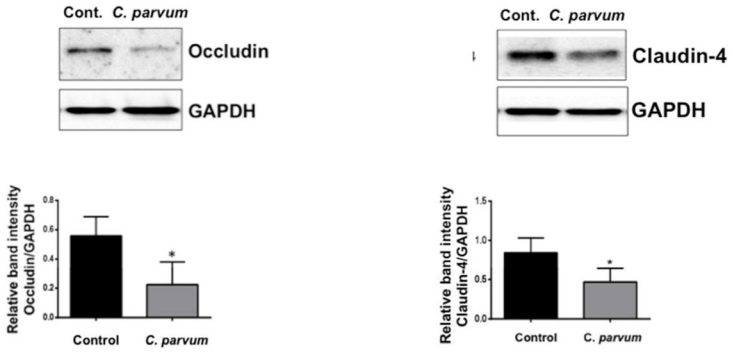

Figure 4C

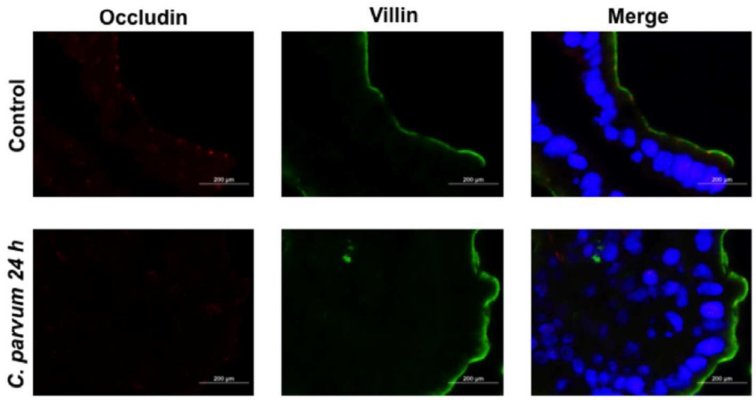

Figure 4C

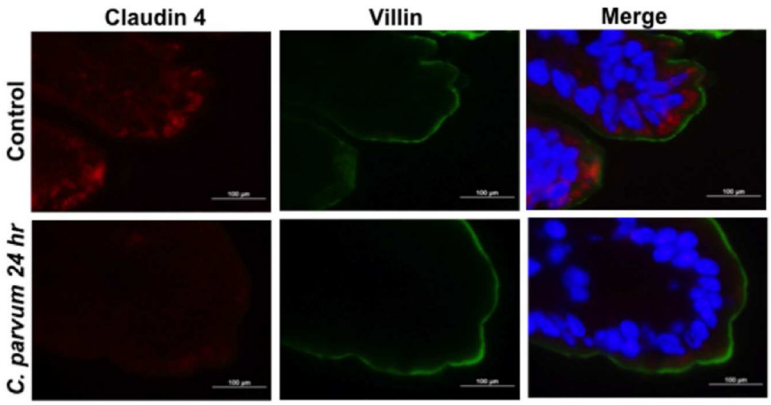

Figure 4C

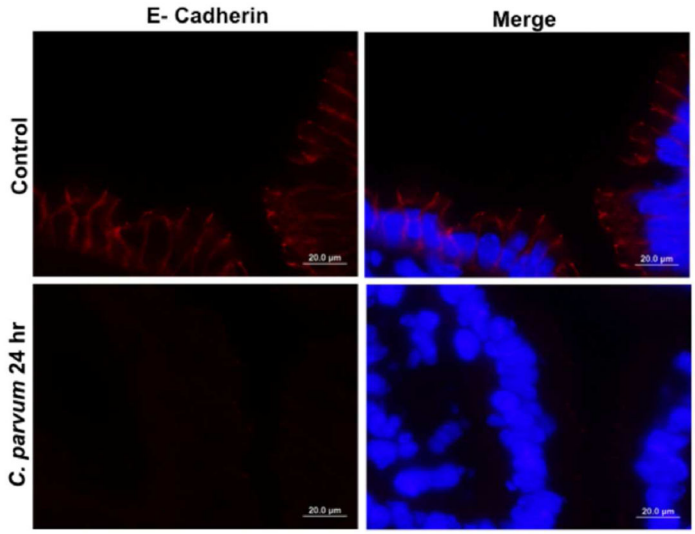

Figure 4.

Effects of *C. parvum* infection on the mRNA and protein levels of occludin, claudin 2, claudin 4 and E-cadherin in mouse ileum and jejunum. (A) Relative mRNA abundance of occludin, claudin 2, claudin 4 and E-cadherin in total RNA samples extracted from scrapped mucosa of jejunum and ileum of control or 24 and 48 hr *C. parvum* infected mice was determined by real-time RT-PCR using gene-specific primers. GAPDH was used as an internal control. Values are mean ± SE. (N = 8; **P*<0.05 vs. control, ***P*<0.001 vs. control). (B) Upper panels: Lysates prepared from scrapped mucosa of ileum of control or 24 hr *C. parvum* infected mice were subjected to SDS-PAGE and probed with occludin and claudin 4 antibodies. Lower panels: Densitometric analysis of relative band intensities with GAPDH as internal control. (C) Immunofluorescence staining of mucosal sections of ileum of control and 24 hr *C. parvum* infected mice for occludin, claudin 4 and E-cadherin (red), villin (green) and DAPI (blue). Representative images of 4–5 independent experiments are shown.

Figure 5A

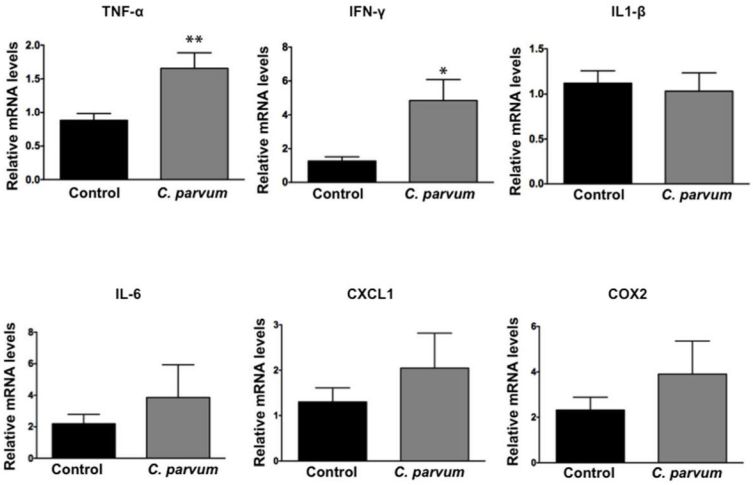

Figure 5B

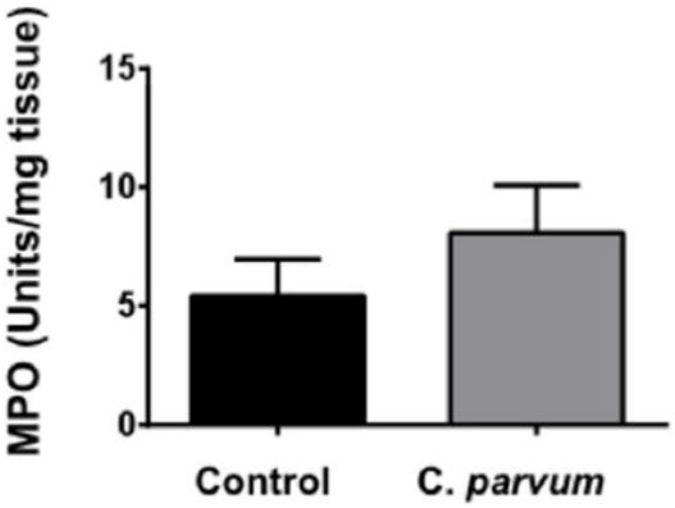

Figure 5C

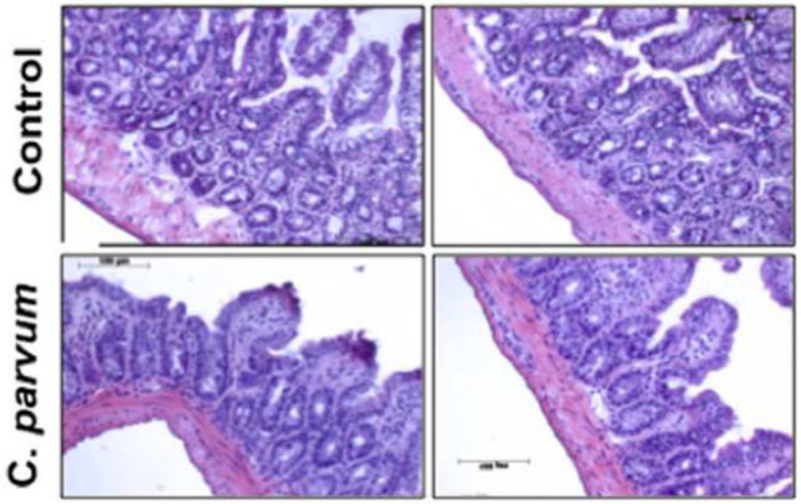

Figure 5.

Effects of *C. parvum* infection on cytokine levels and myeloperoxidase activity in mouse ileum. (A) Relative mRNA abundance of the cytokines (TNF-α, IFN-γ, IL-1β, IL-6, CXCL1 and COX2) in total RNA samples extracted from scrapped mucosa of ileum of control or 24 hr *C. parvum* infected mice was determined by real-time RT-PCR using gene-specific primers. GAPDH was used as an internal control. Values are mean ± SE. (N = 8; **P*<0.05 vs. control, ***P*<0.001 vs. control). (B) MPO activity, measured as described in Methods and calculated as units/g protein are shown as % of control (n = 4). (C) H & E staining of ileal mucosa of control versus 24 hr *C. parvum* infected mice.

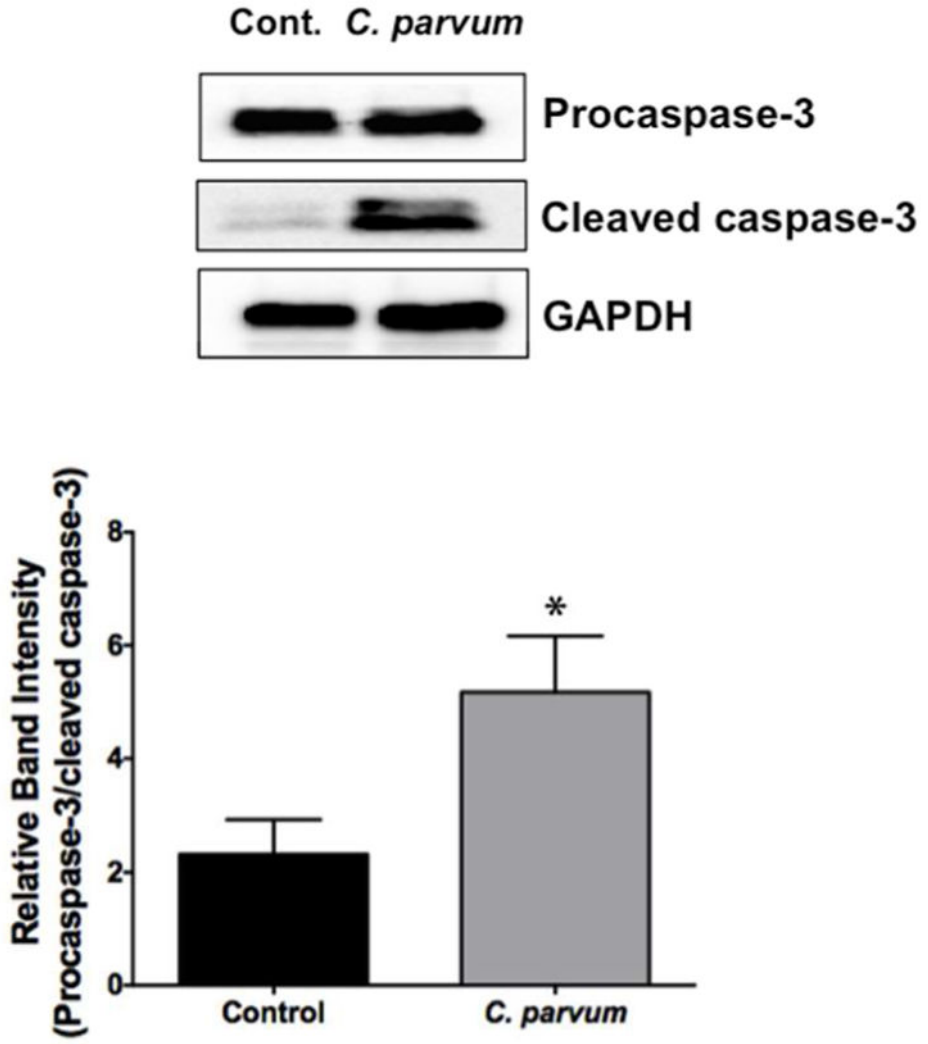

Figure 6.

C. parvum infection induces apoptosis in mouse ileum. Upper panel: Lysates prepared from scrapped mucosa of ileum of control or 24 hr *C. parvum* infected mice were subjected to SDS-PAGE and probed with an antibody that recognized both procaspase-3 and cleaved caspase-3. GAPDH is shown as loading control. Lower panel: Densitometric analysis of the ratio of band intensities of procaspase-3/cleaved caspase-3. Values are mean ± SE. (N = 8; **P*<0.05 vs. control)

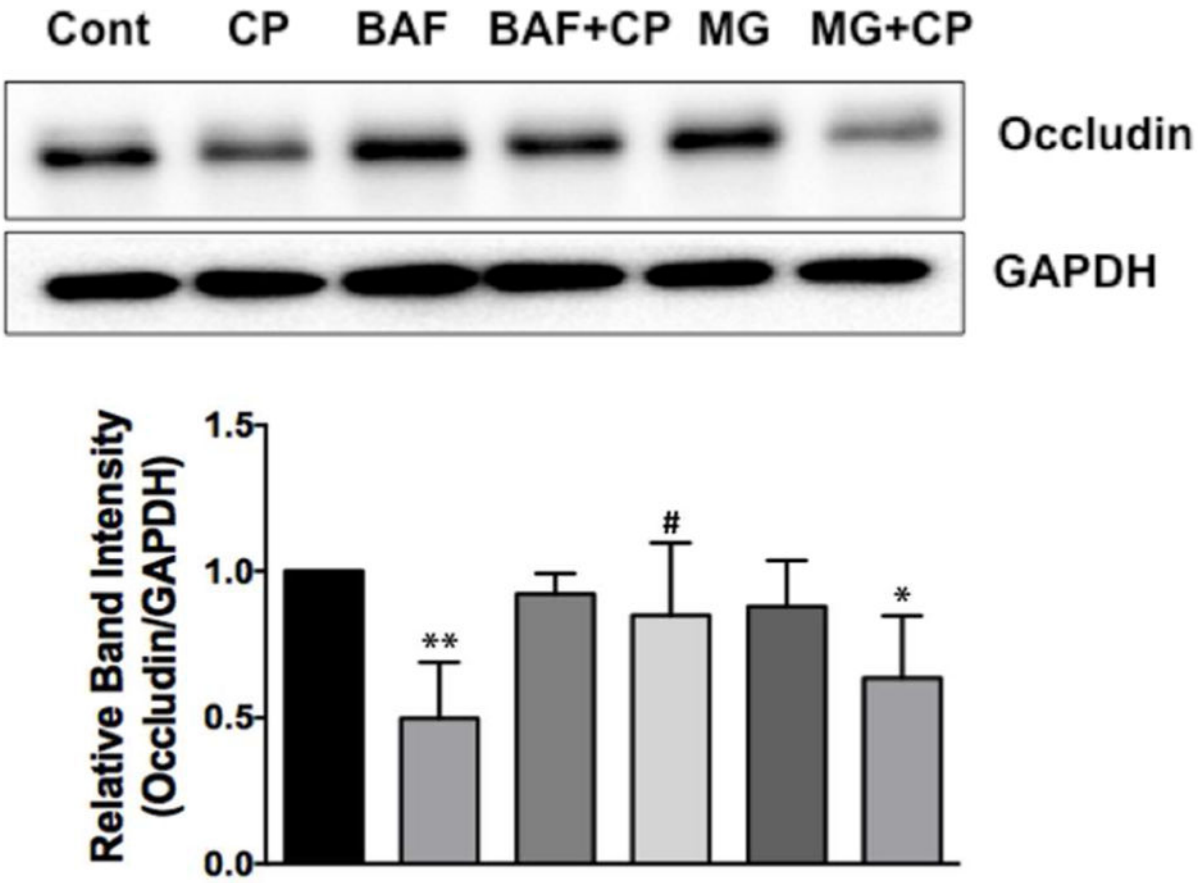

Figure 7.

Bafilomycin A alleviates *C. parvum*-induced downregulation of occludin in Caco-2 cells. Upper panel: Lysates prepared from different groups [control; *C. parvum* with or without bafilomycin A (100 nM) or MG-132 (10 μM); bafilomycin or MG-132 alone] were subjected to SDS-PAGE and probed with anti-occludin antibody in immunoblotting. Lower panel: Densitometric analysis of band intensities in different groups using GAPDH as the internal control. (N=4, ** $P<0.001$ vs. control; # $P<0.05$ vs. CP; * $P<0.05$ vs. control).

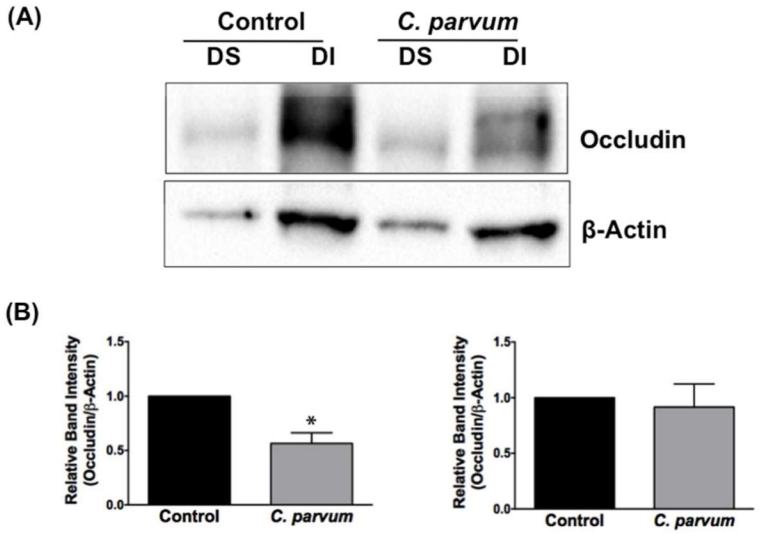

Figure 8.

C. parvum decreases low MW form of Triton-X-100-insoluble occludin. (A) Detergent soluble and insoluble fractions from Caco-2 cell lysates were prepared as described in Methods. Both fractions were subjected to SDS-PAGE and probed with anti-occludin antibody in immunoblotting. A representative image of 3 independent experiments is shown. (B) Densitometric analysis of relative band intensities of low MW (left) and high MW (right) occludin with β-actin as internal control.

Table 1

Gene-specific primers used for real-time PCR analysis of mRNA levels (F: forward primer; R: reverse primer)

Gene	Primer Sequence (5′-3′)
Human occludin	F: CCCCATCTGACTATGTGGAAAGA R: AAAACCGCTTGTCATTCACTTTG
Human claudin 4	F: GGCGTGGTGTTCCTGTTG R: AGCGGATTGTAGAAGTCTTGG
Human E-cadherin	F: ATTTTTCCCTCGACACCCGAT R: TCCCAGGCGTAGACCAAGA
Mouse occludin	F: CCTCCAATGGCAAAGTGAAT R: CTCCCCACCTGTCGTGTAGT
Mouse claudin 2	F: TTAGCCCTGACCGAGAAAGA R: AAAGGACCTCTCTGGTGCTG
Mouse claudin 4	F: AGCAAACGTCCACTGTCCTT R: AATCCACCTCCACCCTTCTT
Mouse E-cadherin	F: CAGCCTTCTTTTCGGAAGACT R: GGTAGACAGCTCCCTATGACTG
Mouse IL-1β	F: GCAACTGTTCCTGAACTCAACT R: ATCTTTTGGGGTCCGTCAACT
Mouse IFN-γ	F: ATGAACGCTACACACTGCATC R: CCATCCTTTTGCCAGTTCCTC
Mouse CXCL1	F: AAAGATGCTAAAAGGTGTCCCCA R: AATTGTATAGTGTTGTCAGAAGCCA
Mouse GAPDH	F: TGTGTCCGTCGTGGATCTGA R: CCTGCTTCACCACCTCTTGAT